Seismic behaviour of circular CFST column to steel beam connections with external diaphragms

Alba A M , Aswathy P

Abstract— This paper deals with the studies conducted on the seismic behaviour of steel beam-to-circular CFST column connections under lateral cyclic loading and constant axial compression. The numerical study is conducted using ANSYS workbench 16.1. The connection failure mainly occurs due to the formation of plastic hinge or shear failure of the panel zone. The shear failure behavior of the panel zone in circular CFST column to steel beam connection in interior columns to steel beam connection is studied in detail. Three different ratios of beam depths (1, 0.75, and 0.5) are considered.models are analysed for varying thicknesses(6mm,8mm,10mm, and 12mm) of column steel tube The equivalent stress distribution, maximum shear stress and load-deflection curves for all the models are evaluated.

Index Terms—Beam to CFST column connection; column steel tube; concrete core; Equivalent stress; External diaphragms;panel zone; Seismic behaviour; Shear behaviour.

1 Introduction

CONCRETE-FILLED steel tubular (CFST) columns have been extensively utilized in high-rise buildings owing to their practical advantages. The tube in a CFST column serves as a convenient formwork for concrete and provides external confinement for the cured concrete. By confining concrete in a CFST column, an increase in the concrete's compressive strength as well as preventing the concrete from spalling can be realized when subjected to overloading. The connections between CFST columns and steel beams are critical elements, and their seismic behavior plays an important role in the security of structural design. With the application of CFST column into engineering practices different types of connection have been developed.

Rigid connection with transverse stiffeners are commonly used and include external diaphragm connection, internal diaphragm connection and through plate connection. In this paper circular CFST column – steel beam connections with external diaphragm connection are modelled and analyzed using finite element software. A typical external diaphragm connection used for CFST column is shown in Figure 1.

Square CFST columns are commonly used beacause of the ease in connection between the beam and column. Eventhough the seismic performance of circular CFST column is better compared to square column; the difficulty in connection makes it less used.

Studies are reported on CFST column steel beam connection by various researchers since 1980. Cyclic load tests are adopted by many researchers to determine the efficiency of the connection. In 2005 Park J W et.al [8] conducted an experimental study on the cyclic performance of wide flange beam square concrete filled tube columns joint with stiffening plates around the column and also described the force transfer mechanism of the connection.

The use of a composite frame with different beam depth ratio can reduce the overall weigth of the frame. The shear behavior and failure mechanisms of composite connection may be different due to the beam depths ratio, so it is essential to assess the applicability of the joint for the beam to CFST column connection with external stiffeners. Figure 3(a) shows a normal composite frame and figure 3(b) shows the composite frame with differences in beam depths.

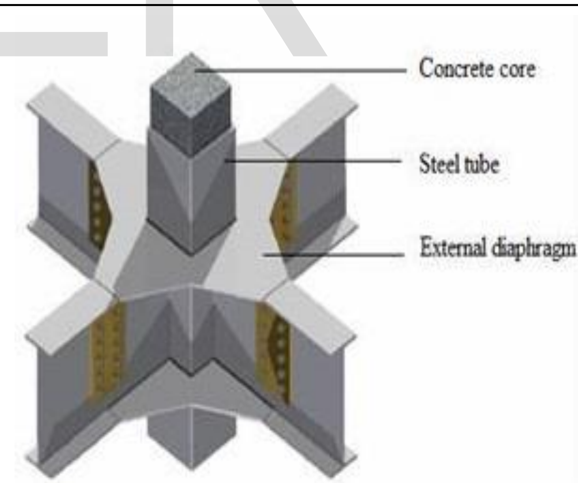

Fig. 1. External Diaphragm connection

This paper presents a finite element models for interior joint of a circular CFST column and steel beam with external diaphragms. The models are used to investigate the effect of thickness of steel tube on the shear behaviour of the joints under applied cyclic displacement at beam end. Three models with varying beam depth ratios are concidered for the analysis. All the models are analysed to study the variation in shear behaviour of the column steel tube and the concrete core by varying the thickness of the column steel tube. The modelling

- *Alba A M is currently pursuing masters degree program in structural engineering in APJ Abdul Kalam Technological University, India. E-mail: alba.akm@mail.com*
- *Aswathy P is currently working as Assistant Professor in Thejus Engineering College , India. E-mail: aswathyvinod08@mail.com*

was done in ANSYS 16.1.

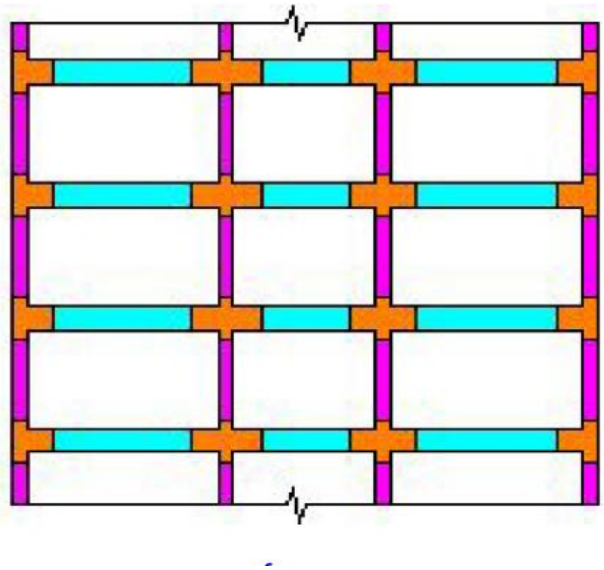

Fig. 3. (a) Normal composite frame

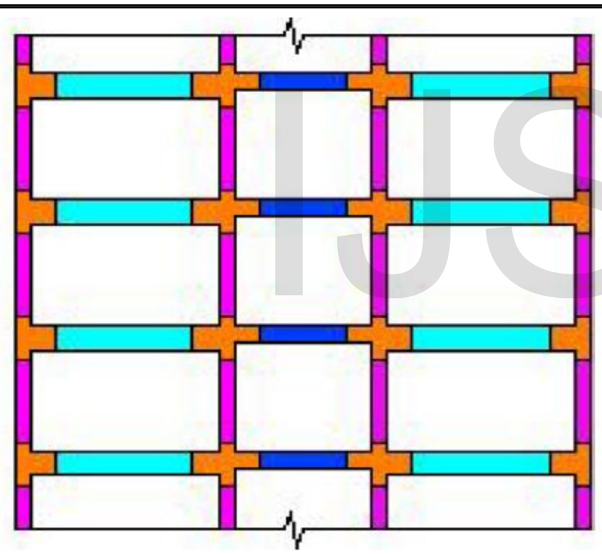

Fig. 3.(b) Composite frame with differences in beam depth.

2 Finite Element Model

2.1 Geometry of the Connection

The interior CFST column to steel beam connection consist of a cicular Concrete Filled stel column of diameter 219 mm with a tube thickness of 6 mm is used to connect the steel beam.the detailed geometry of every part in the connection is given in the table 1. The geometry is adapted from the experimental study conducted by Daxu et.al [1].

2.2 Material Model

The isotropic hardening model is selected for concrete.SOLID65 element with multi-linear stress-strain curve is employed for modelling concrete in the FEA. The confined uniaxial stress-strain curve is applied to define the concrete material property. Tests have been shown that the stress strain

TABLE 1
GEOMETRIC AND MATERIAL PROPERTIES OF SPECIMEN

Specimen		Yield strength (MPa)	Geometry (mm)
I beam	Flange	257	**150×6**
	Web	285	**288×4**
Steel tube		368	**Φ219×6**
Diaphragm		332	**60×6**

relationship for concrete confined by suitable arrangement is different from that of unconfined concrete. For the CFST column a general stress strain curve for confined concrete is suggested by Liang and Fargomeni [8] is used and is shown in Fig.4. The concrete used has an unconfined cube compressive strength of 27.5 MPa. The Poisson's ratio of concrete is taken as 0.2.

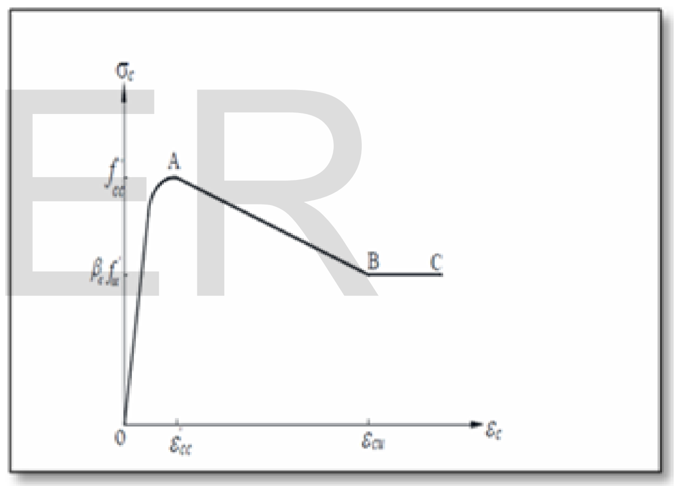

Fig. 4 Stress-strain curve for confined concrete

The commencement of plastic deformation in steel is predicted by von-Mises yield criterion. The von-Mises yield criterion defines the equivalent von-Mises stress σe which is compared with the characteristic yield strength of material to predict yielding.The material properties of the steel specimens used in the connection is given in Table 1.

2.3 Concrete to steel interface Modelling

The interaction between concrete and steel tube at the interface was modeled using contact elements. The outer surface of concrete and inner surface of the steel tube was specified to give a frictional contact. The classical isotropic Coulomb friction model was used to model the interaction assuming the coefficient of friction as 0.6. CONTACT174 and TARGE170 elements are used for modelling this contact.

2.4 Applied Displacements and Loading

An axial compressive load is applied in the column and cyclic displacements are applied at the beam end. The axial compressive load applied to the column was 1300 kN and was kept constant for the whole loading process. Then a cyclic displacement is applied in the beam end the loading pattern is adopted from the experimental study conducted by Daxu et.al in 2012 [1]. The applied displacement and load are given in Fig. 5.

TABLE 2
DETAILS OF MODELS

No.	Steel column (mm)	Beam element	Beam1 (mm)	Beam2 (mm)	d_{b2}/d_{b1}
1. (A)	φ219X6	Flange	150X6	150X6	1
		Web	288X4	288X4	
2. (B)	φ219X6	Flange	150X6	150X6	0.75
		Web	288X4	213X4	
3. (C)	φ219X6	Flange	150X6	150X6	0.5
		Web	288X4	138X4	

TABLE 3
GEOMETRIC SPECIFICATIONS OF MODELS

Model	Diameter of core concrete (mm)	Thickness of steel tube(t) (mm)	Diameter of diaphragm (mm)	Width of diaphragm (mm)
A6	207	6	219	60
A8	207	8	223	60
A10	207	10	227	60
A12	207	12	231	60
B6	207	6	219	60
B8	207	8	223	60
B10	207	10	227	60
B12	207	12	231	60
C6	207	6	219	60
C8	207	8	223	60
C10	207	10	227	60
C12	207	12	231	60

In this model boundary conditions are applied to the top and bottom of the CFST column. At the top surface the displacement in X and Y direction are constrained and at the bottom surface the displacement in X, Y and Z direction are constrained.

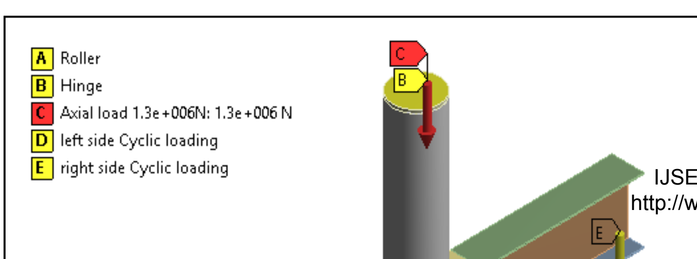

2.5 Specification of Model

A total 5 models are developed varying the thickness of the steel tube in the connection. The material properties for steel tube, diaphragm and beam are kept constant. In the concrete core the confined compressive strength will depend on the D/t ratio of the CFST column.

Three different beam depth ratios 0.5, 0.75,1 were considered for the analysis. The details of the models are given in table 2. The models are named as A, B, C for the beam depth ratios 1, 0.75, 0.5 respectively.The finite element model developed was used to investigate the effect of thickness of stainless steel tube on the shear stress distribution in the connection, column tube and the concrete core. Four different thicknesses (6mm, 8mm, 10mm, and 12mm) were considered for the analysis. The geometric specifications of the mdels for the varying thicknesses are shown in table 3.

3 RESULTS AND DISCUSSIONS

3.1 Equivalent Stress Distribution in Models A6 - A12

For steel the failure criterion adopted is the equivalent Von-Mises yield criterion. For concrete the Principal stress is compared with the compressive strength of concrete since it is a brittle material. The equivalent stress distribution in all the four models A6, A8, A10, and A12 is given in figure 6(a) – (d). As the thickness increases the area under each stress range decreases.

For model A6 the maximum stress occurs in the column. As the thickness of the steel tube increases the area under the maximum stress range also decreases. As the thickness of the steel tube is increased to 12 mm large part of tubes are under the stress range of 50 – 200 MPa.

The yielding is extended to the whole depth of steel beam in all the four models. This significant yielding indicates a plastic hinge formation near to the beam diaphragm joint. Only in model A6 equivalent stress exceeded the yield strength of steel tube.in model A8 – A1 2 the stress induced in tube is lessthan its yield strength and largest part of the tubes are under the stress range of 100 – 200 MPa. so as the thickness of steel tube increases the failure of beam will occur first avoiding the possibility of column failure.

3.2 Equivalent Stress Distribution in Models B6 – B12

The equivalent stress distribution in the models is given in Fig. 7(a) – (d). It is evident from the figure that the maximum stress in the model B6 has decreased slightly as the beam depth ratio is reduced to 0.75. As the thickness increases the area under each stress range decreases. The stress distribution is same as that in models with beam depth ratio one.

The stress distribution range is similar to models A6 – A12. The maximum value of stress occurred in model B6 and the minimum value of stress occurred in model B12, this indicates that maximum stress decreases as the thickness of the column steel tube increases.

3.3 Equivalent Stress Distribution in Models C6 – C12

The equivalent stress distribution in the models is given in Fig. 8(a) – (d). It is evident from the figure that the maximum stress in the model B6 has decreased slightly as the beam depth ratio is reduced to 0.5. As the thickness increases the area under each stress range decreases. The stress distribution is same as that in models with beam depth ratio 1 and 0.75. Model C12, this indicates that maximum stress decreases as the thickness of the column steel tube increases.

Eventhough the stress distribution range is similar to models A6 – A12, the maximum stress values for all the thicknesses is nearer to the maximum stress values obtaines for models with beam depth ratio 0.75. The maximum value of stress occurred in model C6 and the minimum value of stress occurred in model C12, this indicates that maximum stress decreases as the thickness of the column steel tube increases.

The yielding is extended to the whole depth of steel beam in all the four models. This significant yielding indicates a plastic hinge formation near to the beam diaphragm joint. For the model A6 equivalent stress is less than the yield strength of steel tube and largest part of the tubes are under the stress range of 100 – 200 MPa.

3.4 Maximum shear Stress Distribution in concrete core and column steel tube for models

The maximum shear stress in column steel tube and the concrete core is given in table 4. It is evident from the table that the shear stress in column tube reduces as the thickness of the tube increases. This shows that the shear capacity of the column increases as the thickness of the column steel tube increases. Thus the shear behaviour of the connection is enhanced with the increase in column tube thickness.

It can be observed from the table that for all the models the value of maximum shear stress is nearer to 200 MPa. There is only very little difference between the shear stress values. The minimum shear stress value for all the models is near to 150 MPa. The least value of shear stress occurred for the models with beam depth ratio 0.5 and the least value occurred for model C12.

The increase in thickness of the steel tube reduces the stress in the concrete core, this is because of the increased confinement in the concrete. Nearly 50 % of the stress in concrete is reduced when the column thickness is increased to 12 mm, in the case models with beam depth ratio 1 and 0.75. For the model with beam depth ratio 0.5, the stress in concrete is reduced 30 %.

TABLE 4
MAXIMUM SHEAR STRESS IN CONCRETE CORE AND COLUMN STEEL TUBE

Model	Maximum shear stress in column (MPa)	Maximum shear stress in concrete (MPa)
A6	195.61	15.0
A8	174.57	8.43
A10	166.09	7.91
A12	159.08	6.92
B6	188.97	13.19
B8	188.73	8.38
B10	171.1	7.23
B12	160.17	6.76
C6	192.12	9.25
C8	192	7.87
C10	167.95	7.25
C12	152.34	6.76

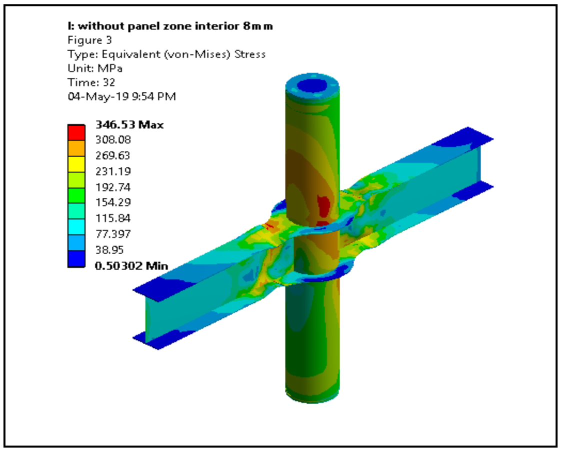

(a) Model A6

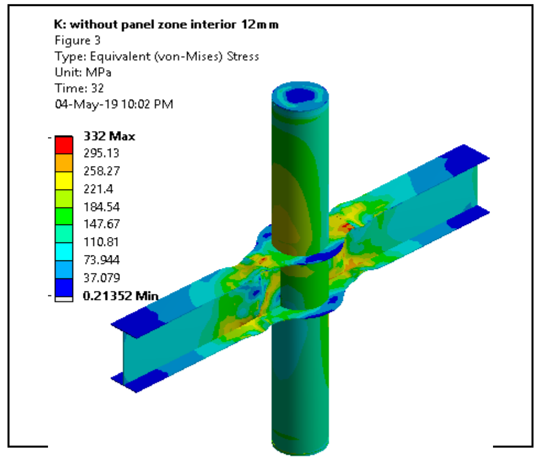

(b) Model A8

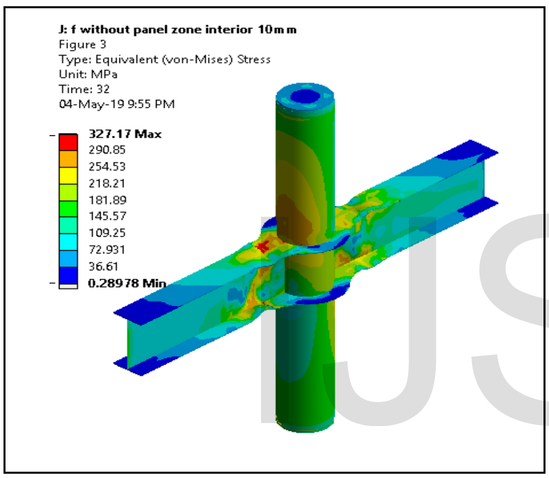

(c) Model A10

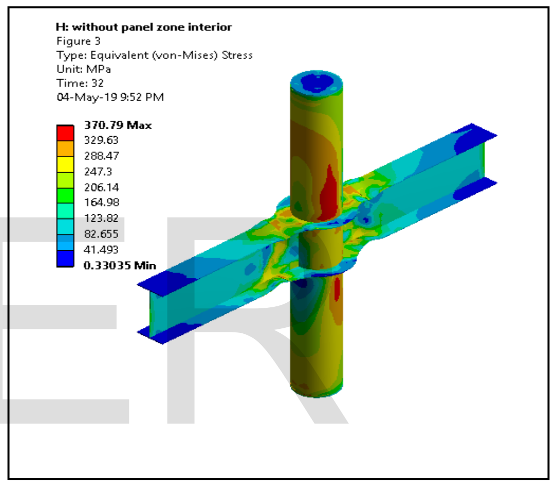

(d) Model A12

Fig. 6 Equivalent stress distribution in models A6 – A12

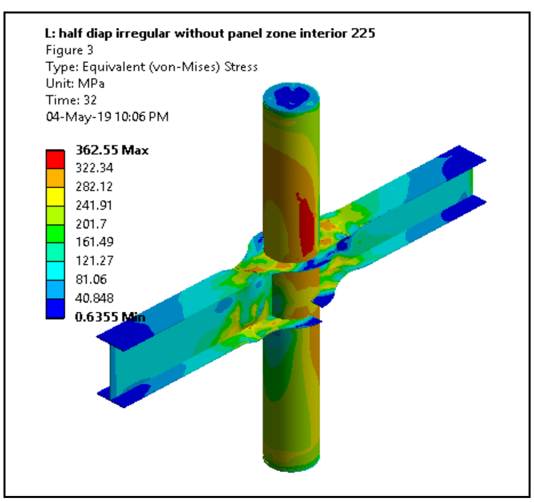

(a) Model B6

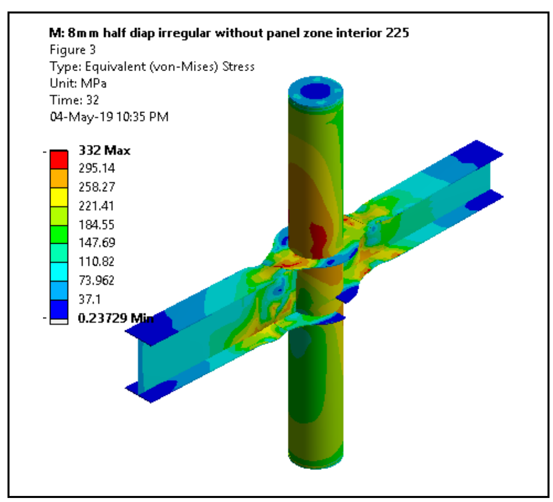

(b) Model B8

Fig. 7 Equivalent stress distribution in models B6 – B8

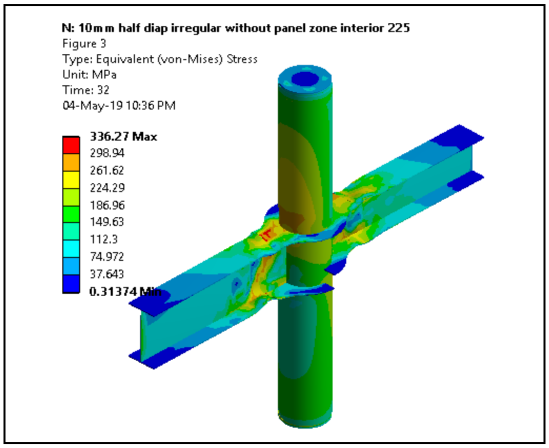

(c) Model B10

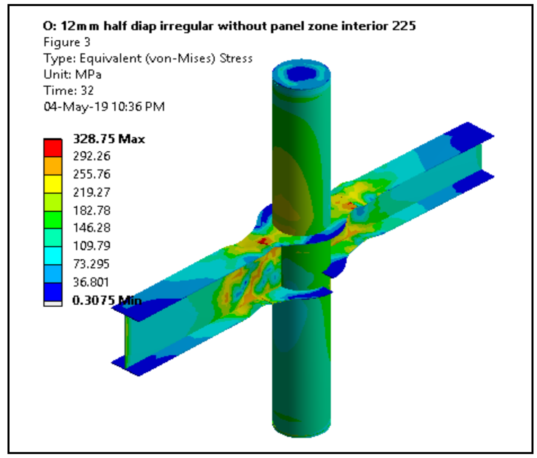

(d) Model B12

Fig. 7(contd) Equivalent stress distribution in models B10 – B12

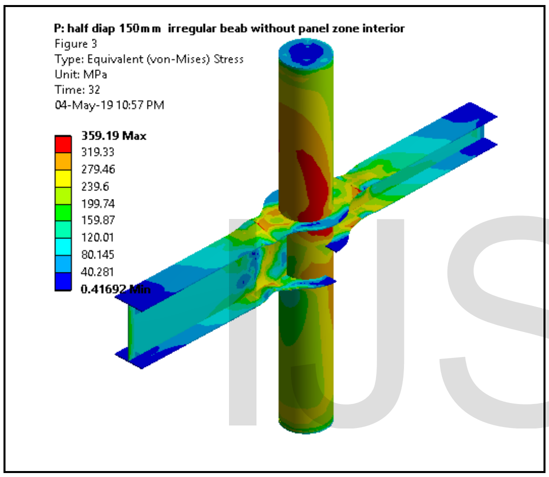

(a) Model C6

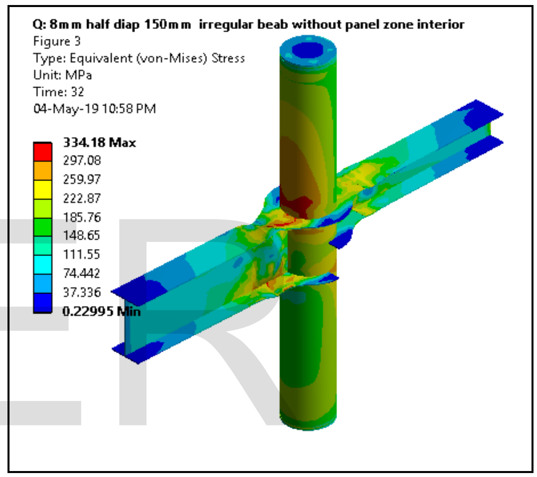

(b) Model C8

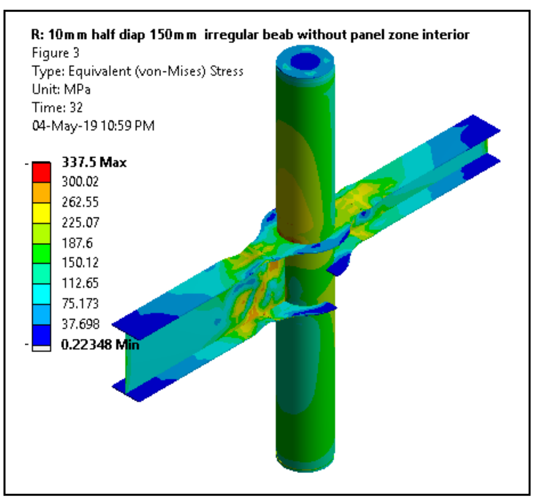

(c) Model C10

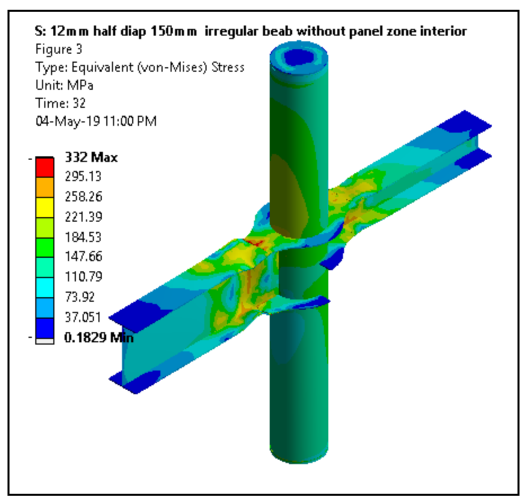

(db) Model C12

Fig. 8 Equivalent stress distribution in models C6 – C12

International Journal of Scientific & Engineering Research Volume 10, Issue 5, May-2019
ISSN 2229-5518

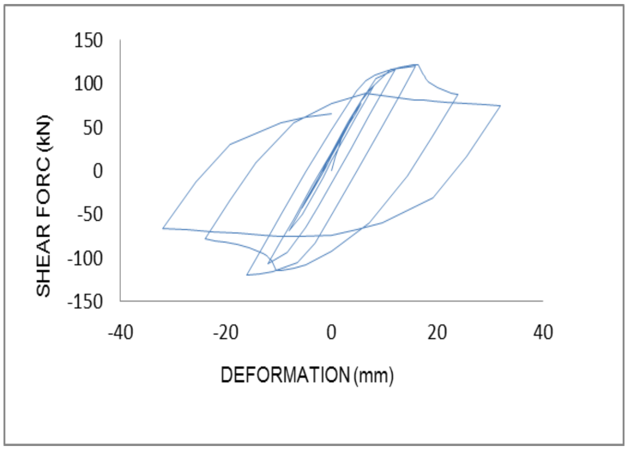

Fig. 9 Load – deformation curve for Model A6

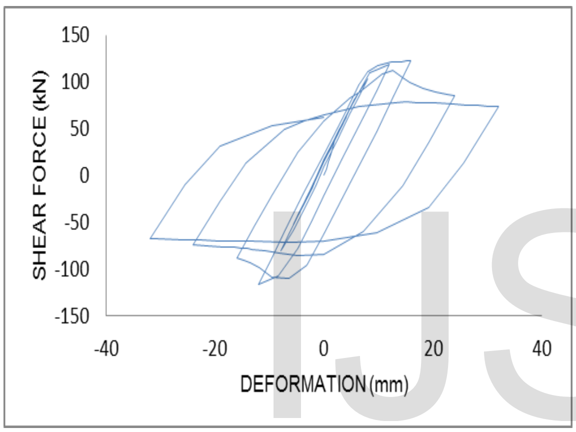

Fig. 10 Load – deformation curve for Model B6

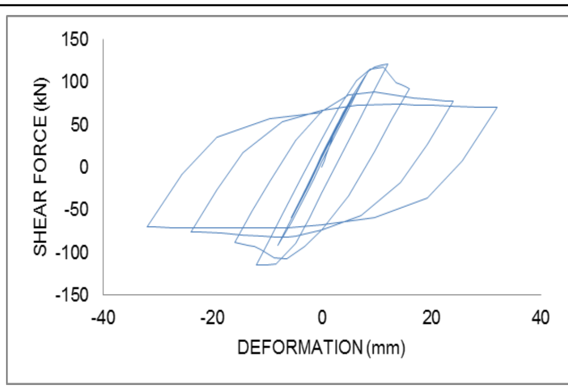

Fig. 11 Load – deformation curve for Model C6

3.5 Shear force – Deformation Hysteretic Curves for Models A6, B6 and C6

The Shear force – deformation hysteretic curves for models A6, B6 and C6 is given Fig.9, Fig.10, and Fig.11 respectively .The hysteretic curves shows that the behaviour of all the models is similiar. It is evident from the figures that the change in beam depth ratios is not affecting the shear behaviour of the connection. All the models showed similar behaviour. The deformation corresponding to maximum shear force is near to 15mm in all the models. It can be observed from the graphs that the maximum force in all the models is between 100kN and 150 kN. The area of the hysteresis curve for all the models is similar.

4. Conclusions

- As the thickness of the tube increases the yielded area in the steel tube decreases
- Stress induced in concrete also decreases as the thickness of the steel tube increases.
- Increase in tube thickness affects the stress distribution of steel tube and concrete
- The beam area nearer to the diaphragm is yielded first
- The thickness of the steel tube should be selected by reducing the probability of column failure and also by considering economy
- The finite element model can be used for parametric studies for the effect of axial load ratio, dimension and shape of stiffener, etc.
- The stress in concrete is reduced due the increased confinement in the concrete due to the increase in column tube thickness.
- All the models showed similar hystertic behaviour. This shows that the differences in beam depths will not severely affect the seismic performance of the connection.
- When beam depth on either sides of the column is different the behaviour of the connection is not severely affected. So reducing the beam depth will effectively reduce the overall weight of the steel structure without affecting the performance of the structure.

5. References

1. **Daxu Zhang, Shengbin Gao, Jinghai Gong (2012), "Seismic behaviour of steel beam to circular CFST column assemblies with external diaphragms",** ***Journal of Constructional Steel Research*** **, 76: 155-166.**
2. **Bin Rong, Shuai Liu, Jia-BaoYan, Ruoyu Zhang (2018), "Shear behaviour of panel zone in through – diaphragm connections to steel tubular columns",** ***Thin walled structures*** **122: 286-299.**
3. **Ben Mou, Yongtao Bai (2018), "Experimental investigation on shear behaviour of steel beam-to-CFST column connections with irregular panel zone",** ***Engineering Structures 168***
4. **Ben Mou, Xi Li, Yongtao Bai, Lisa Wang(2018), "Shear behavior of panel zones in steel beam-to-column connections with unequal depth of outer annular stiffener",** ***Engineering Structures 168***

5. **Ben Mou, Xi Li, Yongtao Bai,Baojie H, V.I. Patel (2018), "Numerical evaluation on shear behavior of irregular steel beam-to-CFST column connections",** ***Journal of Constructional Steel Research*** **, 148**
6. **O. Mirza(2010), "Finite Element Analysis of the Behaviour of Composite Beam-to-Column Connections Subjected To Seismic Loading",** ***2010 Structures Congress © 2010 ASCE***
7. **Chin-Tung Cheng, Lap-Loi Chung(2003), "Seismic performance of steel beams to CFST column connections",** ***Journal of Constructional Steel Research*** **, 59.**
8. **Lin-Hai Han, Wen-Da Wang, Zhong Tao (2011), "Performance of circular CFST column to steel beam frames under lateral cyclic loading",** ***Journal of Constructional steel research*****, 67: 876-890.**
9. **Cristian Vulcu, Aurel Stratan, Adrian Ciutina, and Dan Dubina (2017), "Beam-to-CFT high-strength joints with external diaphragm .ll: Numerical simulation of joint behaviour",** ***journal of structural engineering*****, -1—1**
10. **Ben Mou, Xi Li, Yongtao Bai,Baojie H, V.I. Patel (2018), "Numerical evaluation on shear behavior of irregular steel beam-to-CFST column connections",** ***Journal of Constructional Steel Research*** **, 148.**
11. **Fa-xing Ding, Guo-an Yin, Li-zhong Jiang, Yu Bai (2018), "Composite frame of circular CFST column to steel-concrete composite beam under lateral cyclic loading",** ***Thin walled structures*****, 122: 137-146.**